ELSEVIER

Journal of Alloys and Compounds 216 (1994) 33–38

Journal of ALLOYS AND COMPOUNDS

Low-temperature magnetic susceptibility and resistivity measurements and electron probe microanalysis of $Y_{1-x}U_xPd_3$

J. Xu[a], P.J.C. Signore[a], B. Andraka[a], W.A. Acree[b], M.W. Meisel[a,*], Y. Takano[a]

[a]*Department of Physics and Center for Ultralow Temperature Research, PO Box 118440, University of Florida, Gainesville, FL 32611-8440, USA*

[b]*Major Analytical Instrumentation Center, PO Box 116400, University of Florida, Gainesville, FL 32611-2066, USA*

Received 18 March 1994

Abstract

We have extended the low-temperature magnetic susceptibility and resistivity measurements of $Y_{1-x}U_xPd_3$ ($x \approx 0.2$) down to millikelvin temperatures. One sample showed Curie–Weiss-like paramagnetic susceptibility between 50 mK and 2 K. Another small sample appeared to have nearly constant susceptibility between 400 μK and 120 mK. The signal arising from paramagnetic impurities has been estimated from the susceptibility of undoped YPd_3 measured between 600 μK and 170 mK. No signature of superconductivity was observed in the resistivity measurements down to 5 mK. Electron probe microanalysis showed that the sample composition was modulated on a scale of tens of micrometers.

Keywords: Inhomogeneities; Non-Fermi liquid; Resistivity measurements; Electron probe microanalysis; Magnetic susceptibility

1. Introduction

Heavy-electron metals show many interesting properties in heat capacity, magnetization, electrical resistivity, and superconductivity at low temperatures [1]. In particular, the Pauli-like magnetic susceptibility and the linear heat capacity at low temperature are indicative of Fermi liquid systems. However, some experimental evidence suggests non-Fermi-liquid behavior in alloys of $Y_{1-x}U_xPd_3$ [2–5] and in several other systems [6–9].

The Fermi-level tuning effect in $Y_{1-x}U_xPd_3$, as Y^{3+} is replaced by uranium, suggests that uranium ions are tetravalent [10,11]. It is possible that uranium ions in a cubic crystalline electrical field have a Γ_3 doublet ground state which is non-magnetic [12], as has been suggested by neutron scattering results [13] and by the observation of a weak magnetic field dependence of the heat capacity and the resistivity [3]. From heat capacity [2,4] and muon spin relaxation [14] work, the magnetic phase diagram of $Y_{1-x}U_xPd_3$ has been proposed, and for x of about 0.2, it possesses a boundary between a spin glass phase and a non-magnetic state at low temperature. Although only a single phase with the cubic $AuCu_3$-type crystal structure was found for low uranium concentrations ($0 \leqslant x \leqslant 0.5$) using X-ray diffraction [2], the electron probe microanalysis (EMPA) performed by Süllow et al. [15] found that the uranium concentration is not necessarily uniform and may vary by about 30%. In addition, due to the high melting temperature of about 1700 °C, the inhomogeneities in x cannot be fully removed by annealing the sample for extended periods of time at the highest temperature which is typically achievable in most laboratories, namely 1200–1500 °C. It is conceivable that some of the differences in the data reported by various groups arise from variations in the sample due to fabrication and preparation procedures [16].

In fact, there are considerable differences in magnetic susceptibility and heat capacity of $Y_{1-x}U_xPd_3$ reported by different experimental groups. The observed zero-field heat capacity of $\Delta C/T = -(a/T_K) \ln T$ [2–5] appears to be consistent with the theoretical predictions of the two-channel quadrupolar Kondo effect (QKE) [12,17,18] for $x \leqslant 0.2$. However, the finite residual $T=0$ entropy $S(0) = (R/2) \ln 2$, which is predicted by the two-channel QKE model, has not been directly observed. Furthermore, in specimens with $x \approx 0.2$, the scaling behavior in magnetic field dependent heat capacity, $C(T,H) - C(T,0) = f(H/T^{1.3})T$ cannot be explained by the two-channel QKE model [3]. In addition, the electrical resistivity is predicted to have $\rho(T)/\rho(0) = 1 - b(T/T_K)^n$ with $n = 1/2$ [19]. However, $n \approx 1$ was observed in all the samples measured by various groups [2–5,15] with $\rho(0)$ varying from 140 to 360 μΩ cm.

*Corresponding author.

SSDI 0925-8388(94)01243-B

A pure magnetic two-channel effect [17,18] would yield a temperature dependence of the susceptibility given by $\chi(T) \sim -\ln T$ at low temperatures. On the other hand, for an electrical quadrupolar two-channel Kondo effect, a Van Vleck susceptibility term of $\chi(T) \sim A - BT^{1/2}$ is expected [20]. Using $x \approx 0.2$ specimens, Maple et al. [21] have observed this Van Vleck term in their magnetization data from 0.6 to 40 K and in high magnetic fields, which saturate the impurity magnetization. Their results are fit by the expression $\chi(T) = \chi(0)[1 - \alpha(T/T_K)^{1/2}]$, where $\chi(0) = 5.9 \times 10^{-3}$ emu (mol U)$^{-1}$ and $\alpha T_K^{-1/2} = 0.056$ K$^{-1/2}$. Although no information on the impurity distribution was provided, the amount of their signal coming from magnetic impurities could be fitted by assuming the presence of a 0.1% concentration of holmium with $J = 8$ and $g_J = 0.5$.

Previous susceptibility and resistivity measurements of $Y_{1-x}U_xPd_3$ have focused primarily on the $x \approx 0.2$ system and have been performed down to 0.6 K and 20 mK respectively [5,21]. Initially, our work was motivated by an interest in extending the study of the temperature dependence of the susceptibility over a wider range at low temperatures. Since we observed different temperature dependences of the susceptibility in the millikelvin and microkelvin regimes, resistivity investigations of $Y_{1-x}U_xPd_3$ ($x \approx 0.2$) and susceptibility studies of YPd_3 (and later, our electron microprobe analysis) were performed with the goal of gaining insight into the origin of the difference. In fact, we were motivated to undertake our EMPA work after we had learned about the results of Süllow et al. [15]. Our EMPA results are in qualitative agreement with those reported in that paper. In addition, no evidence for a superconducting transition has been observed down to 5 mK. Consequently, the different temperature behaviors that we have observed in the susceptibility studies may be related to the different excitation fields that were used in the two experiments. The experimental details are described in the next section, which will be followed by a presentation of our results and a discussion of our interpretations, before we summarize in the final section.

2. Experimental details

2.1. Sample preparation

Our polycrystalline $Y_{1-x}U_xPd_3$ ($x \approx 0.2$) and YPd_3 specimens were prepared by arc-melting stoichiometric amounts of the constituent elements in an argon atmosphere. Approximately 200 mg was fabricated in each batch, which was less than the 1 g batches typically made in other laboratories. Smaller masses could conceivably lead to a faster cooling rate after the arc-melting and, consequently, to slightly different compositions when comparing our samples with the larger ones fabricated by other groups. X-ray diffraction analysis found our samples to have a single phase with the $AuCu_3$-type crystal structure and a lattice constant of 4.074 Å [3]. Depleted uranium was used in an attempt to reduce the self-heating in the resultant samples.

2.2. Magnetic susceptibility

The magnetic susceptibility of one sample (3.03 mg) was investigated from 400 μK to 120 mK on Cryostat I in the University of Florida Microkelvin Research Laboratory, while three other pieces, with a total mass of 97.0 mg (55.45 mg, 30.24 mg and 11.32 mg), were studied together from 50 mK to 2 K on a home-made dilution refrigerator operating in the main physics building. In order to establish the possible effect that trace amounts of magnetic impurities might have on the ultra-low temperature susceptibility results of our $Y_{1-x}U_xPd_3$ ($x \approx 0.2$) samples, the susceptibility of a 23.6 mg specimen of YPd_3 has also been measured from 600 μK to 170 mK.

The susceptibility measurements of the 3.03 mg $Y_{1-x}U_xPd_3$ ($x \approx 0.2$) sample and the YPd_3 specimen were performed with an a.c. mutual inductance bridge operating at 16 Hz with an rms excitation field of 40 nT, using a d.c. superconducting quantum interference device (SQUID) as a null detector. The size of the sample was chosen to minimize self-heating which might prevent the material from being cooled into the microkelvin temperature range. A schematic overview of the experimental tower is shown in Fig. 1. Four Ag wires (diameter 0.76 mm) (Marz grade from Materials Research Corporation, Orangeburg, NY 10962, USA. Typical results of emission spectroscopy (all in ppm): Al = 3, Bi < 3, Cu < 2, Fe < 3, Mg < 2, Ni < 2, Pb < 3, Si < 3, Sn < 2, V < 1) were welded into a Ag base which was bolted to the top of a Cu nuclear demagnetization stage. The sample to be studied was attached with

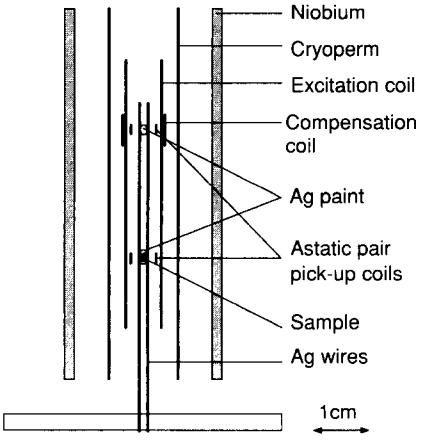

Fig. 1. Schematic of the experimental tower of the ultra-low temperature experiment.

silver paint (Catalog number P3100 from Johnson Matthey, Materials Technology, Royston, Herts, UK. The Ag component (54% by weight), contains Fe up to 1000, typically 200–800, Ni typically < 500, and other metallic impurities < 100 (all in ppm)) to the Ag wires in the region of the lower pick-up coil. A roughly equal amount of silver paint was placed on the Ag wires in the region of the upper pick-up coil. In order to avoid temperature-dependent background signals arising from the excitation and pick-up coils and the shields (see Fig. 1), this assembly was heat sunk to the mixing chamber which was maintained at a constant temperature during the measurement. A room temperature mumetal shield was wrapped around the cryostat when the Nb shield was cooled through its superconducting transition. The mumetal–Nb–Cryoperm (Cryoperm 10 from Vacuumschmelze GmbH, Hanau, Germany) combination reduced the remnant background static magnetic field to about 20 nT [22]. The size and the sign of relative changes in susceptibility values as a function of temperature, $\Delta\chi(T)$, were calculated from the geometry of the sample and the coil, and this procedure has been used successfully in other experiments [22]. Owing to an offsetting background signal which was larger than the signal arising from the sample by a factor of approximately 2×10^3, absolute susceptibility values could not be obtained. In other words, only relative magnetic susceptibility values, $\Delta\chi(T)$, may be extracted from the measurement. The contributions from the Ag wires and the silver paint were largely compensated by the astatic pick-up coil arrangement, and our previous work did not observe a measurable signal arising from them [22]. An upper bound on the temperature sweep was determined by the point ($\sim$170 mK) where the heat switch between mixing chamber and Cu nuclear stage starts to conduct significantly.

The magnetic susceptibility of the 97 mg $Y_{1-x}U_xPd_3$ sample, which consisted of the three pieces as described earlier, was studied from 50 mK to 2 K using standard mutual inductance techniques operating at 317 Hz, with an rms excitation field less than 10 μT in the earth's magnetic field. The temperature-dependent background of the detection assembly has been measured separately and has been subtracted from the results. Absolute $\chi(T)$ values were obtained by normalizing the data to the results of Andraka and Tsvelik [3] between 1.8 and 2.0 K, the temperature range where the data sets overlapped.

2.3. Electrical resistivity

As will be discussed in the next section, the diamagnetic trend that we observed in ultra-low temperature susceptibility was unexpected. In order to test if this behavior might be associated with a superconducting transition, we made a four-lead a.c. resistivity measurement on yet another, cylindrically shaped $Y_{1-x}U_xPd_3$ ($x\approx0.2$) sample with a diameter of 0.9 mm, length of 4 mm, and mass of 25 mg. The sample was glued with GE 7031 varnish to a Cu plate which was bolted onto the Cu nuclear stage. A piece of cigarette paper served as electrical isolation between the sample and the Cu plate. Four leads were spot-welded to the sample and varnished to the Cu plate through the paper over a length of about 3 cm to provide additional thermal contact for the sample. The sample assembly was covered with a Cu radiation shield which was thermally anchored to the Cu nuclear stage. Since no magnetic-field shielding was used, the sample was exposed to the earth's field. During the course of the run, the principal excitation frequency and rms level were nominally 25 Hz and 0.2 μV. At lowest and highest temperatures, the bridge excitation frequency and level were varied from 2.5 Hz to 2.5 kHz and by a factor of 10, respectively. In both instances, there was no effect on our results. The Joule heating due to probing excitation was about 5 pW at the lowest temperature, a factor of 4 smaller than the radioactive self-heating of the sample. Various reasonable estimates for the heat load into the sample and for its thermal anchoring are consistent with the measurements achieving a minimum temperature of 5 ± 1 mK when the Cu cold-plate was at 3.83 ± 0.05 mK as measured by a ^{3}He melting curve thermometer.

2.4. Electron probe microanalysis

In the summer of 1993, Süllow et al. [15] shared their work with us, and their results motivated us to undertake our EPMA studies. More specifically, in an attempt to understand the data that will be presented in the next section, we examined all of our $Y_{1-x}U_xPd_3$ specimens with EPMA, using a commercial Jeol 733 system. Finally, this work was complemented through the use of a standard optical microscope with 400× magnification.

3. Results

Our magnetic susceptibility data for the 97 mg specimen are shown in Fig. 2, where the error bars reflect an uncertainty in the subtraction of the background and in the calibration of the signal to the results of Andraka and Tsvelik [3]. The data may be least-squares fitted to a Curie–Weiss-like expression, $\chi(T)=\chi(0)+C/(T-\theta)$, for $T<2$ K, and the result is shown as a solid line in Fig. 2, where $\chi(0)=(7.6\pm0.2)\times10^{-3}$ emu (mol U)$^{-1}$, $\theta=-21\pm2$ mK, and $C=(7.0\pm0.1)\times10^{-3}$ emu K (mol U)$^{-1}$, which implies the effective magnetic moment of about 0.24 μ_B per uranium ion. The susceptibility increased faster at low temperature than it did at high temperature where $\chi(T)\approx0.013\ (T/\mathrm{K})^{-0.3}$

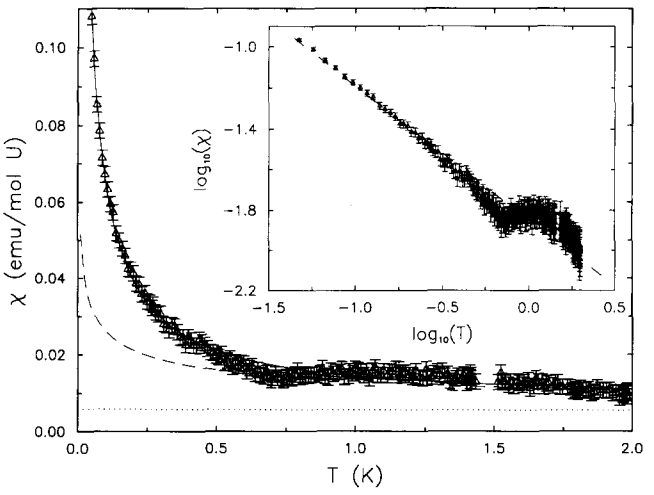

Fig. 2. Magnetic susceptibility of the 97 mg $Y_{1-x}U_xPd_3$ ($x \approx 0.2$) sample as a function of temperature. The error bars reflect the uncertainty resulting from the subtraction of the background signal and from the calibration procedure used to obtain absolute emu (mol U)$^{-1}$ units (see text). The solid line represents a Curie–Weiss fit to the data and the fitting parameters are given in the text. The dashed line represents the $\chi(T) = 0.013\ (T/\mathrm{K})^{-0.3}$ emu (mol U)$^{-1}$ reported by Andraka and Tsvelik [3]. The Van Vleck paramagnetic susceptibility, $\chi(T) = (5.9 \times 10^{-3}$ emu (mol U)$^{-1}$) $[1 - 0.056\ (T/\mathrm{K})^{1/2}]$, reported by Maple et al. [21] is shown as the dotted line. The inset shows the $\log_{10}(\chi)$ vs. $\log_{10}(T)$ where χ is in units of emu (mol U)$^{-1}$, and T is in units of K. The dash-dot line shows the results of a fit to the simple expression $\chi(T) \propto T^k$, where $k = -0.66$.

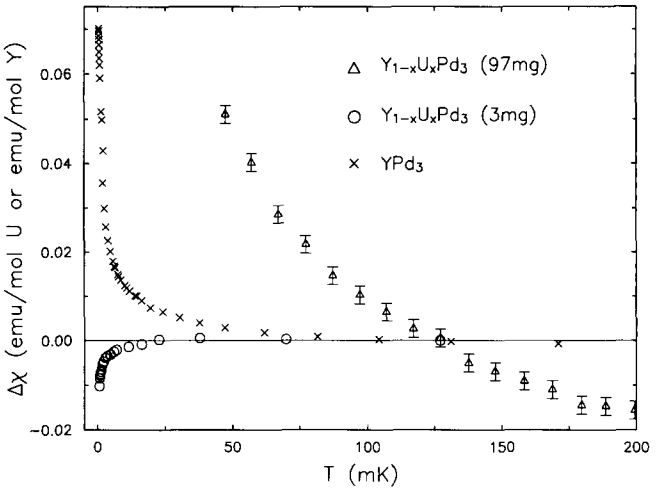

Fig. 3. Relative magnetic susceptibility, $\Delta\chi(T) = \chi(T) - \chi(125\ \mathrm{mK})$, as a function of temperature. The results for the $Y_{1-x}U_xPd_3$ ($x \approx 0.2$) sample are in units of emu (mol U)$^{-1}$ while the data for YPd_3 are in units of emu (mol Y)$^{-1}$.

emu (mol U)$^{-1}$ [3], as indicated by the dashed line in Fig. 2. For comparison, the Van Vleck paramagnetic susceptibility, $\chi(T) = (5.9 \times 10^{-3}$ emu (mol U)$^{-1}$) $[1 - 0.056\ (T/\mathrm{K})^{1/2}]$, reported by Maple et al. [21] is shown in Fig. 2 as the dotted line. Finally, the inset of Fig. 2 enables one to compare our results with those reported in Ref. [15], and a simple fit of our data to $\chi \propto T^k$ is shown by the dash-dot line with $k = -0.66$.

The relative changes of the susceptibility, $\Delta\chi(T) = \chi(T) - \chi(125\ \mathrm{mK})$, for the 3.03 mg $Y_{1-x}U_xPd_3$ ($x \approx 0.2$) sample and the YPd_3 specimen are shown in Fig. 3. In addition, $\Delta\chi(T)$ for the results shown in Fig. 2 are reproduced in this figure. Surprisingly, the 3.03 mg sample exhibited a nearly constant signal in the temperature region overlapping that of the 97 mg specimen, whose susceptibility was strongly temperature-dependent. In addition, a small diamagnetic trend in the susceptibility was present in the 3.03 mg sample at very low temperature. By way of comparison, the susceptibility of a 23.6 mg YPd_3 sample, which was made from the same starting materials as the $Y_{1-x}U_xPd_3$ specimens, is shown in Fig. 3. Since YPd_3 is a non-magnetic compound, its susceptibility allows for a reasonable estimate of the impurity contribution to the susceptibility of our $Y_{1-x}U_xPd_3$. The susceptibility of the YPd_3 reference can be fitted to a Curie–Weiss form, and a least-squares fit yields $C = (1.44 \pm 0.01) \times 10^{-4}$ emu K (mol Y)$^{-1}$ and $\theta = -1.62 \pm 0.02$ mK. Since the impurity analysis[1] shows that most of the magnetic impurities come from Y, the susceptibility of the reference should be scaled by the molar fraction of Y in the sample to yield an estimated impurity contribution $C = (7.20 \pm 0.05) \times 10^{-4}$ emu K (mol U)$^{-1}$, which is a factor of 10 smaller than the Curie constant for the 97 mg sample.

Between 5 mK and 200 mK, the resistivity of our $Y_{1-x}U_xPd_3$ ($x \approx 0.2$) was constant within 0.2%, with $\rho(0) \approx 260\ \mu\Omega$ cm. Our measurements at higher temperature agree with those reported by other workers [2–5,15]. No evidence of a superconducting transition was observed down to 5 mK. We cannot resolve the predicted $n = 1/2$ term in $\rho(T)/\rho(0) = 1 - b(T/T_K)^n$ since our signal-to-noise ratio of about 10^3 was not sufficient.

A typical back-scattered electron image is shown in Fig. 4, which displays the results of the 55.45 mg fragment of the 97 mg sample. Although our results are in qualitative agreement with those of Süllow et al. [15], our samples seem to have larger average grain size and a greater variation of x. Typically, two types of grains are observed. One type of grain is long and narrow, with characteristic lengths in excess of 100 μm and widths of approximately 20 ± 10 μm. These needle-like objects fill local regions of the sample by being parallel to grains with the same geometry. The second type of grain is smaller and rather irregularly shaped, and these objects appear to be interrupted versions of the needle-like grains. Consequently, they have a characteristic width which is similar to the needle-like grains, but their typical lengths vary from 10 to 50 μm. Within

[1] Pure metals commercially available from Johnson Matthey. Yttrium contains: Gd = 50, Lu = 3, Nd = 10, Sc = 2, Tl = 1, Al = 50, Cu = 10, Fe = 20, Si = 1. Uranium contains: Cu < 1, Fe = 7, Mo < 1, Ni < 1, Si = 30, Ti < 1, Zr < 1. Palladium contains: Pb = 3, Fe = 2, Cu < 1, Mg < 1, Si < 1, Ag < 1. All impurity contents are in ppm.

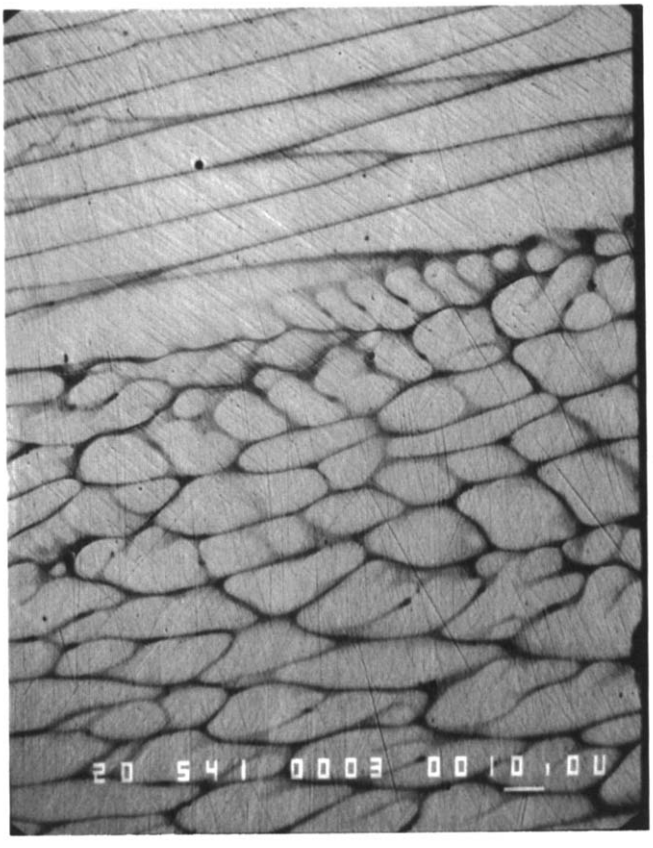

Fig. 4. Back-scattered electron image of the 55.45 mg sample of $Y_{1-x}U_xPd_3$ ($x \approx 0.2$). The electron energy is 20 keV, and the marker represents 10 μm. The needle-like regions are clearly distinguishable from the smaller, irregularly shaped areas as discussed in the text. Within the resolution of the technique, all of our $Y_{1-x}U_xPd_3$ ($x \approx 0.2$) specimens gave qualitatively the same type of back-scattered images.

the resolution of the technique, all of our $Y_{1-x}U_xPd_3$ specimens gave qualitatively the same type of back-scattered images as the one shown in Fig. 4.

In Fig. 4, the somewhat remote possibility that the dark regions are cavities between the lighter grains has been eliminated by optical microscopy. In other words, the contrast shown in the figure represents the concentration variation of uranium which back-scatters electrons more strongly than yttrium. The composition, which was determined by comparing the X-ray wavelength dispersive spectrum to the pure element standard, was found to be $x = 0.063 \pm 0.008$ in the darkest regions and $x = 0.25 \pm 0.01$ in the brightest areas. The fact that the total atomic counts added up to 100% is consistent with the optical microscopy which showed a flat single surface with no cavities. The variation of concentration in our sample is larger than the variation of $0.14 \leqslant x \leqslant 0.23$ measured by Süllow et al. [15].

4. Discussion

One may ask why the susceptibility results of our small and large samples do not agree, especially in view of the fact that the EPMA studies showed no difference between the 97 mg and the 3.03 mg specimens. However, this probing technique cannot provide information about the possible existence of impurities at levels below 0.1% (for typical accumulation times of 10 to 100 s for each element) or about their distribution at length scales of less than 1 μm. It is possible, although unlikely, that our two samples have different impurity concentrations and distributions. Holmium impurities in a concentration as large as that postulated by Maple et al. [21] are unlikely to be present in our sample in view of the purity of our starting materials. Our relatively large susceptibility in the 97 mg sample suggests that there was a small amount of 'free' uranium ($< 1\%$) ions ($\approx 3\ \mu_B$). It is somewhat disturbing that the susceptibility of the 3.03 mg sample did not indicate the same behavior as that measured in the 97 mg specimen, and, furthermore, the paramagnetic contribution from the impurities associated with the yttrium (as estimated from the YPd_3 study) was not observed. In fact, the 3.03 mg sample possessed a diamagnetic trend at the lowest temperatures.

The most significant difference between the measurement of our 97 mg and 3.03 mg samples is that they were performed with different a.c. excitation levels and that one study was performed in the earth's magnetic field whereas the other was in a nominally zero field (< 20 nT). Of course, the difference in the results may be related to background effects. Whereas the millikelvin measurements measured a background contribution in a separate run with the sample absent, the ultralow temperature studies rely on parasitic magnetic contributions coupling equally to both coils of the asatic pair configuration. For example, the Ag wires should not present a significant problem since they contain a low level of impurities (see Section 2.2.), and their contribution to the signal was balanced to better than 1%. On the other hand, it is possible that the diamagnetic trend in the susceptibility of the 3.03 mg $Y_{1-x}U_xPd_3$ ($x \approx 0.2$) sample at ultralow temperature is an artifact due to an overcompensation by the silver paint in the upper astatic pick-up coil. However, we did not observe any significant effect arising from the silver paint in previous work using a similar experimental tower and a sample that was more than 200 times larger in magnetic moment strength [22]. Therefore, the exact mechanism causing the two samples to have different responses remains to be further investigated.

5. Summary

In summary, we have measured the magnetic susceptibility of $Y_{1-x}U_xPd_3$ ($x \approx 0.2$) samples to 600 μK and electrical resistivity to 5 mK, where no evidence of a superconducting transition was observed. Although

further work is needed, the difference in susceptibility between our 97 mg and 3.03 mg samples is most likely due to the different excitation and remnant static fields present for the measurements. Finally, our EPMA results indicate that the samples possess uranium-deficient ($x=0.063\pm0.008$) and uranium-rich ($x=0.25\pm0.01$) regions which vary throughout the specimens on the scale of tens of micrometers.

Acknowledgments

We gratefully acknowledge discussions with M.B. Maple, J.A. Mydosh, C.L. Seaman and S. Süllow, and in particular, we thank S. Süllow and J.A. Mydosh for sharing their work prior to publication. Various forms of support from the members of the UF Microkelvin Research Laboratory are deeply appreciated. This work was supported, in part, by the NSF under Grants DMR-8902538 (JX and YT), DMR-9200671 (PJCS and MWM), DMR-9208866 (BA) and INT-9214239 (MWM).

References

[1] D.W. Hess, P.S. Riseborough and J.L. Smith, in G.L. Trigg, E.S. Vera and W. Greulich (eds.), *Encyclopedia of Applied Physics*, VCH Publishers, New York, 1993, p. 435.
[2] C.L. Seaman, M.B. Maple, B.W. Lee, S. Ghamaty, M.S. Torikachvili, J.-S. Kang, L.Z. Liu, J.W. Allen and D.L. Cox, *Phys. Rev. Lett., 67* (1991) 2882.
[3] B. Andraka and A.M. Tsvelik, *Phys. Rev. Lett., 67* (1991) 2886.
[4] C.L. Seaman, M.B. Maple, B.W. Lee, S. Ghamaty, M.S. Torikachvili, J.-S. Kang, L.Z. Liu, J.W. Allen and D.L. Cox, *J. Alloys Comp., 181* (1992) 327.
[5] H.R. Ott, E. Felder and A. Bernasconi, *Physica B, 186–188* (1993) 207.
[6] B. Andraka and G.R. Stewart, *Phys. Rev. B, 47* (1993) 3208.
[7] H. Amitsuka, T. Hidano, T. Honma, H. Mitamura and T. Sakakibara, *Physica B, 186–188* (1993) 337.
[8] B. Andraka, *Physica B*, 1994, in press.
[9] D.A. Gajewski, P. Allenspach, C.L. Seaman and M.B. Maple, *Physica B*, 1994, in press.
[10] J.-S. Kang, J.W. Allen, M.B. Maple, M.S. Torikachvili, W.P. Ellis, B.B. Pate, Z.-X. Shen, J.J. Yeh and I. Lindau, *Phys. Rev. B, 39* (1989) 13 529; L.Z. Liu, J.W. Allen, C.L. Seaman, M.B. Maple, Y. Dalichaouch, J.-S. Kang, M.S. Torikachvili and M.A.L. de la Torre, *Phys. Rev. Lett., 68* (1992) 1034.
[11] J.W. Allen, L.Z. Liu, R.O. Anderson, C.L. Seaman, M.B. Maple, Y. Dalichaouch, J.-S. Kang, M.S. Torikachvili and M.L. de la Torre, *Physica B, 186–188* (1993) 307.
[12] D.L. Cox, *Phys. Rev. Lett., 59* (1987) 1240; D.L. Cox, *Physica B, 186–188* (1993) 312.
[13] H.A. Mook, C.L. Seaman, M.B. Maple, M.A.L. de la Torre, D.L. Cox and M. Makivic, *Physica B, 186–188* (1993) 341.
[14] W.D. Wu, A. Keren, L.P. Le, G.M. Luke, Y.J. Uemura, C.L. Seaman, Y. Dalichaouch and M.B. Maple, *Physica B, 186–188* (1993) 344.
[15] S. Süllow, T.J. Gortenmulder, G.J. Nieuwenhuys, A.A. Menovsky and J.A. Mydosh, *J. Alloys Comp., 215* (1994) 223.
[16] H.R. Ott and Z. Fisk, in D.R. Salahub and M.C. Zerner (eds.), *The Challenge of d and f Electrons, ACS Symposium Series 394*, American Chemical Society, Washington, DC, 1989, p. 260.
[17] A.M. Tsvelik, *J. Phys. C, 18* (1985) 159.
[18] P.D. Sacramento and P. Schlottmann, *Phys. Lett. A, 142* (1989) 245.
[19] I. Affleck and A.W.W. Ludwig, *Nucl. Phys. B, 352* (1991) 849; ibid., *360* (1991) 641; A.W.W. Ludwig and I. Affleck, *Phys. Rev. Lett., 67* (1991) 3160.
[20] D.L. Cox and M. Makivic, *Physica B*, 1994, in press.
[21] M.B. Maple, C.L. Seaman, D.A. Gajewski, Y. Dalichaouch, V.B. Barbetta, M.C. de Andrade, H.A. Mook, H.G. Lukefahr, O.O. Bernal and D.E. MacLaughlin, *Physica B*, 1994, in press.
[22] O. Avenel, J. Xu, J.S. Xia, M.-F. Xu, B. Andraka, T. Lang, P.L. Moyland, W. Ni, P.J.C. Singore, C.M.C.M. van Woerkens, E.D. Adams, G.G. Ihas, M.W. Meisel, S.E. Nagler, N.S. Sullivan, Y. Takano, D.R. Talham, T. Goto and N. Fujiwara, *Phys. Rev. B, 46* (1992) 8655.